ASIAN JOURNAL OF FORESTRY
Volume 10, Number 1, June 2026
Pages: 12

E-ISSN: 2580-2844
https://doi.org/10.13057/asianjfor/r100115

Urban flood susceptibility and riparian vegetation using GLM-based spatial modelling from vegetation cover in Samarinda, Indonesia

IKHSAN FIQRA NAUFALIANTO[1,♥], MUHAMMAD IQBAL NUR MADJID[2], MUHAMMAD RAFII NUR FAUZAN[1], ABDUL RAHMAN SIDIQ[1]

[1]Faculty of Forestry and Tropical Environment, Universitas Mulawarman. Gunung Kelua Campus, Samarinda 75119, East Kalimantan, Indonesia. Tel.: +62-541-749068, Fax.: +62-541-735379, ♥email: ikhsannaufalianto@fahutan.unmul.ac.id

[2]Department of Forest Management, Faculty of Agriculture, Universitas Sebelas Maret. Jl. Ir. Sutami 36A, Surakarta 57126, Central Java, Indonesia

Manuscript received: 15 December 2025. Revision accepted: 13 February 2026.

Abstract. *Naufalianto IF, Madjid MIN, Fauzan MRN, Sidiq AR. 2026. Urban flood susceptibility and riparian vegetation using GLM-based spatial modelling from vegetation cover in Samarinda, Indonesia. Asian J For 10 (1): r100115. https://doi.org/10.13057/asianjfor/r100115*. Urban flooding in tropical cities is increasingly shaped by land-cover change, yet the contribution of urban vegetation to flood susceptibility remains poorly quantified. This study mapped flood susceptibility in Samarinda, Indonesia, using a Generalized Linear Model (GLM) fitted to 123 spatially thinned flood-presence points derived from georeferenced online reports and 1,000 pseudo-absence points (1:8). Open-source covariates were derived from Sentinel-2 and SRTM, including Enhanced Vegetation Index (EVI), elevation, and built-up occurrence frequency. After screening for multicollinearity and selecting the best minimal model, flood occurrence was negatively associated with EVI and elevation and positively associated with built-up frequency. Model discrimination was high (AUC = 0.959 in a 70/30 split) and remained consistent under spatial block cross-validation, with predictions interpreted as relative susceptibility rather than event-based hydrological simulation. Predicted high susceptibility was concentrated along low-lying river corridors and densely built zones, whereas vegetated and elevated areas exhibited lower susceptibility. Jenks classification indicated 4.74% of the study area in the high class. These findings highlight the importance of maintaining urban vegetation cover, particularly urban riparian forests and green belts, as a nature-based component of flood-risk reduction. The susceptibility map can be used as a consideration for urban forestry planning by prioritizing riparian forest conservation and restoration in river-corridor segments with high predicted susceptibility.

Keywords: Crowd-sourced data, flood susceptibility, Generalized Linear Model (GLM), urban flood, urban riparian forest

INTRODUCTION

Flooding is a hydrometeorological phenomenon that occurs worldwide, particularly in developing countries (Singh 2018). Climate change intensifies this risk through increasingly unpredictable and extreme rainfall, thereby increasing flood likelihood in many regions (Tabari 2020), including urban areas (Fowler et al. 2021; Dharmarathne et al. 2024; Tang et al. 2024). Urban landscapes are heterogeneous mosaics but are commonly dominated by human-made patches (Etter et al. 2011; Zhou et al. 2014; Meili et al. 2021). A defining feature is the prevalence of impervious surfaces-settlements, such as public or commercial buildings, roads, and other infrastructure, whose concentration follows activity intensity and population density (Pickett et al. 2001; Bagan and Yamagata 2015; Imam and Indu 2018). Hydrologically, imperviousness reduces infiltration and increases surface runoff, elevating flood probability during high precipitation events (Jacobson 2011; Du et al. 2015; Zhou et al. 2017).

Urban flood susceptibility is influenced by more than imperviousness alone. The condition, continuity, and management of urban forestry elements, especially riparian forests and vegetated river corridors, also shape how stormwater is slowed, stored, and conveyed during extreme rainfall. As linear buffers adjacent to channels, riparian vegetation can function as hydrological retention space and moderate runoff connectivity, thereby influencing local flood peaks (Olokeogun et al. 2020; Stutter et al. 2021). Riparian corridors are also key green infrastructure because they directly interface with drainage networks and support both hydrological and ecological functions. Conversion of riparian vegetation to impervious land near rivers can exacerbate local flood risk, particularly when discharge increases and overflow occurs (Croke et al. 2017; Kingsbury-Smith et al. 2023). Riparian zones can also serve as refugia for biological communities in urban landscapes (Ehrenfeld and Stander 2010; Guo et al. 2019; Zhang et al. 2022). Riparian vegetation loss may therefore reduce ecosystem quality and weaken urban resilience to hydrometeorological hazards (Cao and Natuhara 2019; Blum et al. 2020).

Vegetation is a key component that maintains the stability of ecosystem services in urban landscapes (Liu and Zhang 2025; Nunes et al. 2025). In a hydrological context, the presence and distribution of vegetation cover are closely related to rainfall, runoff, and flooding events (McGrane 2016; Song et al. 2020; Dowtin et al. 2023; Anys and Weiler 2024). Landscapes with better vegetation cover generally have higher buffering capacity than areas dominated by impervious surfaces (Jacobson 2011; Berland et al. 2017). Thus, the pattern, extent, and configuration of

vegetation cover have the potential to serve as indicators of a region's natural ability to mitigate flood risk (Su et al. 2018; Wu et al. 2020).

A conceptual mechanism links these drivers in urban-riparian systems. Impervious surfaces increase runoff volume and shorten travel time to channels, while elevation controls flow convergence and the tendency for water to accumulate in low-lying areas. Vegetation increases roughness, interception, and infiltration, lowering effective runoff and slowing overland flow. Connected riparian corridors provide buffering and temporary retention along the drainage network, jointly reducing peak flows and flood occurrence during extreme rainfall (Olokeogun et al. 2020; Stutter et al. 2021).

Many flood vulnerability studies still emphasize hydrological and infrastructural drivers, while vegetation and riparian corridor functions are less often quantified in urban susceptibility analyses (Setiawan et al. 2020; Dimaputri et al. 2022; Pallathadka et al. 2022; Ghozali et al. 2024; Agus et al. 2025). Spatially explicit flood-event inventories also remain scarce in many developing-country cities (Nkwunonwo et al. 2020; Dasallas et al. 2024). Studies in Samarinda, Indonesia and comparable tropical cities frequently rely on descriptive remote sensing of land-cover change or input-intensive hydrological modelling, leaving limited evidence on the relative contribution of vegetation, built-up areas, elevation, and water-related proximity at the city scale. Integrating open-source covariates with crowd-sourced flood observations provides a practical and interpretable way to address this gap.

Samarinda, the capital of East Kalimantan Province, is a densely populated city that frequently experiences flooding (Amri et al. 2020; Anwar et al. 2021). Land cover conversion from natural vegetation to built-up areas during 1994-2022 (Agus et al. 2023), including along the Mahakam River corridor and its tributaries (Kedhaton and Krismondo 2024), underscores the relevance of an ecological perspective in flood assessment. This study applies a Generalized Linear Model (GLM) using open-source spatial covariates and crowd-sourced flood-event data derived from spatially interpretable social media reports, following Smith et al. (2017). Therefore, to clarify the quantitative role of vegetation in urban flood dynamics, this study tests the hypothesis that vegetation cover and elevation are negatively associated with flood occurrence, whereas frequency of occurrences of water bodies increases flood susceptibility in urban landscapes. Specifically, we examine whether remotely sensed vegetation indicators, together with topographic and frequency of occurrences of hydrological variables, significantly predict spatial patterns of flood susceptibility in Samarinda.

MATERIALS AND METHODS

Study area

This research was conducted in Samarinda, East Kalimantan (Figure 1), in August to September 2025. Located along the Mahakam River, Samarinda is one of the supporting cities for the sustainability of Indonesia's new capital, Nusantara. Geographically, Samarinda is located at 0°21'1"-0°9'16" South Latitude and 116°15'16"-117°24'16" East Longitude. Rainfall intensity in Samarinda ranges from 111-224 mm per month (BMKG 2021). Ecologically, Samarinda represents urban-riparian interactions in humid tropical regions because it has a clear landscape gradient from relatively low and flood-susceptible river corridors to higher areas (Gunawan et al. 2013; Widayati 2018; Amri et al. 2020) that are generally more vegetated. Samarinda has an elevation ranging from 10 to 200 meters above sea level (masl) (Amri et al. 2020).

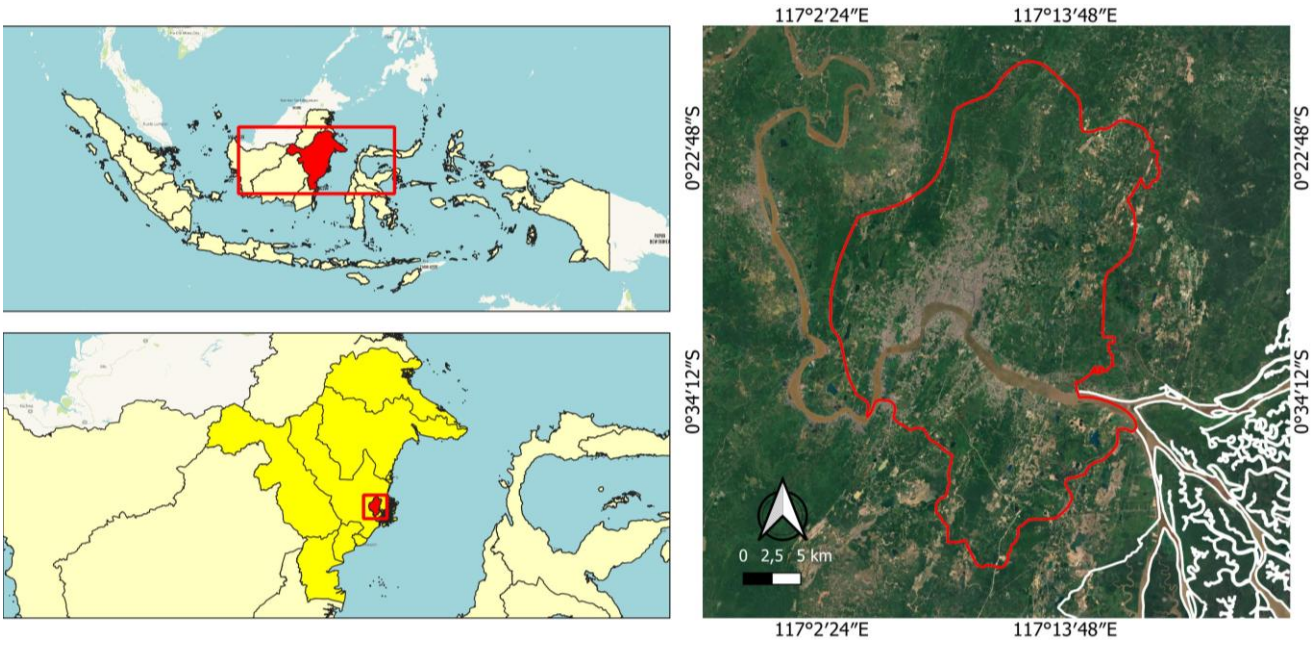

Figure 1. Study location map in Samarinda, East Kalimantan, Indonesia

Elevationally, the study area is dominated by low-to-moderate terrain based on the DEM classification used in this study. Areas below 10 masl constitute 32.56% of Samarinda, while 16.43% lies within 10-20 m. Elevations of 20-50 m account for 31.90%, and elevations above 50 m represent 19.11%. This distribution indicates that 48.99% of the study area lies below 20 masl, supporting the characterization of Samarinda as a river-influenced city with extensive lowland zones potentially susceptible to inundation along the Mahakam River corridor and its tributaries. The landscape mosaic of Samarinda City is also characterized by relatively less green open space compared to built-up areas in the urban landscape (Bhaskara and Pratomo 2023). Land cover classification indicates that built-up areas account for 14.6% of Samarinda City, while vegetation cover reaches 75.61% (based on the administrative boundary). Samarinda is a city traversed by the Mahakam River, with the Northern part of the river (Northern Samarinda) covering the subdistricts of Sungai Kunjang, Samarinda Ulu, Samarinda Utara, Sungai Pinang, Samarinda Kota, Samarinda Ilir, and Sambutan. Meanwhile, the southern part of the Mahakam River (Southern Samarinda) includes the subdistricts of Loa Janan Ilir, Samarinda Seberang, and Palaran.

Data sources

Flood event data was obtained from an online crowd-sourced platform covering the period 2024-2025. In this study, a flood event was operationally defined as a report indicating temporary surface inundation in the urban environment (e.g., roads or residential areas) that was visually evident in videos or corroborated by local media and could be confidently geolocated. Because these crowd-sourced reports do not provide consistent rainfall intensity information, no rainfall-based threshold or severity criterion was applied. Hence, the modelling results are interpreted as relative susceptibility based on documented events rather than as rainfall-triggered predictions for specific storms. The main sources used were georeferenced social media posts containing location information (Smith et al. 2017) and additional verified reports from local media. Data sources from social media were generally in the form of videos, so that locations could be visually identified through street signs or shop signs with the help of Google Street View (Lombardo et al. 2025). Non-georeferenced or ambiguous recordings were excluded to ensure spatial accuracy, and each flood event point (presence) was re-verified using a high-resolution basemap to minimize geolocation errors.

Because flood locations are collected from georeferenced online sources and social media reports, the resulting presence data is inherently susceptible to reporting bias, which tends to be higher in densely populated environments and areas with good connectivity. This bias was not detrimental to the main objective of the analysis because the primary goal of this study was not to estimate the absolute frequency of an event, in this case, flooding, but rather to assess the direction and strength of the association between events and environmental covariates (Ghosh and Dewanji 2016). Consequently, the modeling results are interpreted as relative risk or spatial ranking (Tsumita et al. 2025). To further clarify the modelling design, pseudo-absence points were generated by random sampling within the administrative boundary of Samarinda City used as the study area extent. Nevertheless, the social media data-based approach is considered appropriate for cities with limited real-time flood monitoring systems, as it is able to capture a wider range of flood events reported by the community (Brown et al. 2021).

The locations of flooding events from various online sources were first manually digitized as presence points in the Geographic Information System (GIS) platform, namely QGIS. The resulting presence dataset was then analyzed with spatial thinning using the spThin package in R (Aiello-Lammens et al. 2015) to minimize excessive clustering. Spatial thinning was applied by setting a minimum distance between points using the nearest-neighbor method, so that presence locations were not too close together in one area. This procedure followed common practices in the use of spatial thinning and minimum nearest-neighbor distance to reduce spatial bias in the presence data in point-based modeling (Boria et al. 2014; Aiello-Lammens et al. 2015). The thinning distance was determined by considering the spatial resolution of environmental covariates extracted from Sentinel-2 imagery (10 m), so that nearby presence points did not simply replicate information from the same covariate pixels or directly adjacent pixels. Urban population density was not used as a bias covariate, and no explicit bias surface (e.g., population density or accessibility) was modelled beyond spatial thinning, hence, potential residual reporting bias from online sources is acknowledged. After the spatial thinning process, 123 flood presence points in the form of point vectors were then used for modeling.

Environmental covariates were extracted from open-source datasets. River network data were obtained from the Indonesian Topographic Map (Rupa Bumi Indonesia, RBI), while topographic information was extracted from the NASA SRTM 30 m Digital Elevation Model (Farr et al. 2007) and resampled to match the 10 m spatial resolution of Sentinel-2 imagery. Sentinel-2 Level-2A imagery (cloud cover <10%) with a recording period from January 2024 to September 2025 was used to compile land cover maps using the Random Forest algorithm in Google Earth Engine (Phan et al. 2020; Hasan et al. 2022). Land cover classification includes five classes: built-up, vegetation, bare land, shrubland, and water bodies. The confusion matrix and Kappa coefficient were used to assess the accuracy of the land cover map (Günlü et al. 2009), with an overall accuracy of 0.91 and a Kappa coefficient of 0.88, respectively. From the land cover data, four covariates, namely built-up area, vegetation cover (vegetation and shrubland combined), bare land, and water bodies, were extracted, and then their frequency of occurrence was calculated using the CircAn tool in Biomapper (Hirzel et al. 2004). Vegetation cover was also represented by the Enhanced Vegetation Index (EVI), which was calculated from the same Sentinel-2 composite. All spatial layers were

standardized to a uniform coordinate system (WGS 84/UTM Zone 50 S) prior to spatial statistical modeling.

Data processing and analysis

Flood event points are treated as presence (value=1), while pseudo-absence points (value=0) are randomly generated within the study area to represent non-flooded conditions. A total of 1,000 pseudo-absence points were randomly generated for sampling within the Samarinda urban area. Pseudo-absence sampling was constrained to non-water pixels by masking permanent water bodies using the water-body occurrence layer prior to random point generation, so that background points were not placed on permanent water surfaces. With 123 flood presence points, a prevalence ratio of approximately 1:8 was obtained, which is within the prevalence ratio range (approximately 1:5 to 1:10) commonly used in spatial distribution modeling (Lobo and Tognelli 2011; Barbet-Massin et al. 2012; Gomez et al. 2015; Tong et al. 2023). This approach assumes that most unsampled locations in the study area did not experience reported severe flooding during the study period, while acknowledging that some unreported flood-susceptible locations may still exist. The use of a relatively large number of pseudo-absences can improve model accuracy and reduce overprediction when event data are limited, making this strategy suitable for modeling the probability of an event occurring (Lobo and Tognelli 2011; Barbet-Massin et al. 2012). Therefore, model predictions should be interpreted as relative differences in flood vulnerability across different parts of the city, rather than as absolute probabilities of flooding.

Before proceeding to the model development stage, the environmental variables obtained were first analyzed using Pearson Correlation to minimize multicollinearity. Variable pairs with Pearson correlation coefficients exceeding 0.7 ($|r|>0.7$) or less than −0.7 ($|r|<-0.7$) were considered to have a strong correlation and were not included simultaneously in the model (Brun et al. 2020). The correlation structure among predictors was visualized using the corrplot package version 0.95 in R to facilitate interpretation and variable screening (Wei and Simko 2024). The model was built using the GLM framework with a binomial error distribution or logistic regression approach because this framework provides an explicit and interpretable relationship between the probability of an event occurring and its covariates or predictors (Austin 2007; Neuhaus and McCulloch 2011). Compared to more flexible but black-box approaches, logistic regression can provide relatively simple information about the direction and magnitude of predictor effects through model coefficients, and supports transparent interpretation for future planning and decision-making needs (Rudin 2019).

In the model development stage, a backward stepwise elimination procedure was applied following Crawley (2013) framework, by gradually removing insignificant predictors until the best minimal model was obtained. Because stepwise procedures can inflate Type 1 Error, p-values were interpreted conservatively, and emphasis was placed on effect direction and predictive performance when reporting results. The best minimal model performance was evaluated using the Area Under Curve (AUC) of the Receiver Operating Curve (ROC) based on a random division of 70% presence and pseudo-absence points for model training and 30% for testing (El-Haddad et al. 2021; Liu et al. 2023). The AUC value was calculated with the provision that a value above 0.7 was interpreted as an acceptable model (Robin et al. 2011). Sensitivity and specificity were also calculated at the optimal threshold identified by the Youden index to provide an additional, threshold-based description of classification performance. Effect sizes were further summarized using Odds Ratios (OR) with 95% Confidence Intervals (CI), calculated by exponentiating model coefficients and their corresponding confidence limits for meaningful unit changes in each predictor. Model performance was additionally assessed using spatial block cross-validation to reduce optimistic bias from random splits in spatial data, hence, the dataset was partitioned into spatially separated folds and the AUC was averaged across folds. For descriptive mapping, the continuous susceptibility predictions were reclassified into three classes (low, moderate, high) using Jenks natural breaks, and the percentage area in each class was quantified (Ekeanyanwu et al. 2022; Varra et al. 2024). In addition, the Variance Inflation Factor (VIF) was calculated on the final model to ensure that there was no collinearity between covariates. An acceptable VIF value does not exceed 5, following the practical rule proposed by James et al. (2021). All analyses were performed in R Studio using the terra version 1.8-86 (Hijmans 2025), ggplot2 (Wickham 2016), dplyr version 1.1.4 (Wickham et al. 2023), pROC (Robin et al. 2011), and car (Fox and Weisberg 2018).

RESULTS AND DISCUSSION

Selection and spatial distribution of environmental variables

The Pearson correlation analysis results graph (Figure 2) shows the strength and direction of the correlation between the environmental variables obtained, where the color intensity represents the correlation value. There are eight variables tested in the correlation analysis, including freq_bl (frequency of bare land occurrence), freq_bu (frequency of built-up area occurrence), elev (elevation based on Digital Elevation Model/DEM), EVI, freq-veg_cov (frequency of vegetation cover occurrence), freq_wb (frequency of water bodies), Normalized Difference Built-up Index (NDBI), and eu_riv (Euclidean distance to rivers). There is a strong correlation that has the potential to cause multicollinearity, including between EVI and freq-veg_cov with a value of $|r|=0.84$; NDBI and freq_bu with a value of $|r|=0.72$; freq_bu and freq-veg_cov with a value of $|r|=-0.71$; EVI and NDBI with a value of $|r|=0.7$; and elev and eu_riv with a value of $|r|=0.7$. Other variable pairs showed correlation coefficients below the threshold ($|r|<0.7$).

Based on the Pearson correlation screening ($|r|$ threshold), five predictors were retained for subsequent model development. Those variables consist of EVI, elevation, bare land frequency of occurrences, built-up

frequency of occurrences, and water-body frequency of occurrences. Table 1 presents the predictor variables that will be used in model development.

EVI in Figure 3.A shows variations in the condition of vegetation cover across Samarinda City, with relatively heterogeneous values distributed across different parts of the city. The bare land frequency map in Figure 3.B and the built-up area frequency in Figure 3.C show different spatial patterns, where built-up frequency of occurrences were higher in the central parts of the city and along the Mahakam River corridor, whereas bare land frequency of occurrences were higher in peripheral areas. The elevation map in Figure 3.D illustrates the topographic gradient from the lowlands around the river corridor to higher areas in other parts of the city. Moreover, the water body map in Figure 3.E shows the emergence of water bodies that predominantly follow the course of the Mahakam River and its tributaries. Overall, Figure 3 presents five selected spatial covariates in raster format used as input in the development of the flood susceptibility model.

Flood susceptibility model and predictor significance

After the backward stepwise variable elimination, the best minimal model used for flood susceptibility assessment consisted of three variables (Table 1). These variables were EVI, elevation, and built-up area. All variables included in the model had *p*-values below 0.01. The EVI or vegetation cover (-5.338±1.268, $p \leq 0.001$) and elevation (-0.063±0.007, $p \leq 0.01$) showed negative associations with flood occurrence. In contrast, flood occurrence was positively associated with built-up area (0.042±0.022, $p \leq 0.001$). Effect-size estimates expressed as odds ratios indicated that a 0.1 increase in EVI reduced flood odds (OR=0.59, 95% CI: 0.45-0.75), a 10 m increase in elevation reduced flood odds (OR=0.53, 95% CI: 0.33-0.79), whereas a 10% increase in built-up frequency increased flood odds (OR=1.52, 95% CI: 1.33-1.78).

High flood susceptibility values appear to be concentrated along the Mahakam River corridor, particularly in the central-western zone of the city and several areas in the northern part of the study area. On the other hand, lower flood susceptibility values are more dominant in the southern part and several parts of the periphery in Samarinda City. Higher predicted susceptibility values were mapped near the Mahakam River corridor, with lower values in areas farther from the main channel. Figure 4.A shows the continuous spatial prediction of flood susceptibility produced by the best minimal GLM, while Figure 4.B presents the same surface reclassified into three classes. For descriptive reporting, the reclassification indicates that low susceptibility covers 617.28 km² (89.33%) of the study area, moderate susceptibility covers 40.92 km² (5.92%), and high susceptibility covers 32.78 km² (4.74%).

Table 1. The best minimal model for flood susceptibility

Flood occurrence~EVI+Elevation+Built-up, Res.Dev=235.91, df=780				
Parameter	**Slope**	**Std.Error**	**Z Value**	**P-Value**
Intercept	-2.311	0.729	-3.167	1.54e-03**
EVI	-5.338	1.268	-4.21	2.55e-05***
Elevation	-0.063	0.007	-2.858	4.27e-03**
Built-up	0.042	0.022	5.764	8.2e-09***

Note: Res.Dev: Residual Deviance, df: Degree of Freedom, *: p-value≤0.05, **: p-value≤0.01, ***: p-value≤0.001

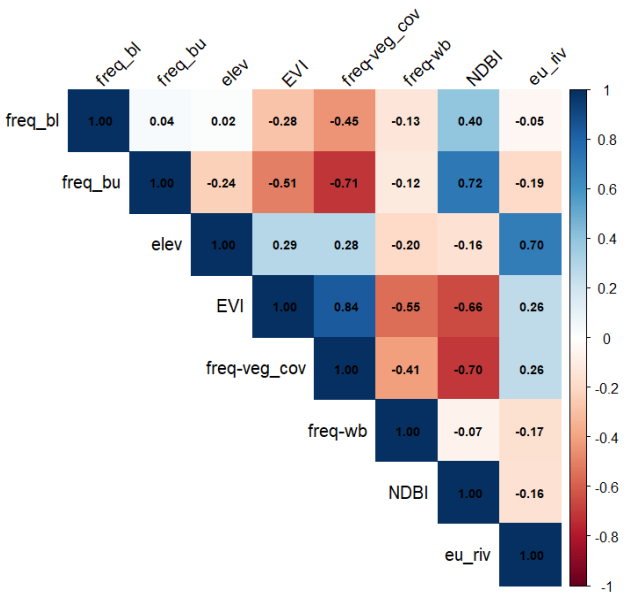

Figure 2. Pearson correlation coeficient matrix of eight environmental variables gathered from an open source resources. The color gradient represents the strength and direction of correlation, where blue indicates positive and red indicates negative relationships

Table 2. List of variables for model building

Abbreviation	**Description**
EVI	Vegetation index calculation with Sentinel-2 imagery
elev	Elevation from DEM extracted from NASA SRTM (Farr et al. 2007) that resampled into Sentinel-2 pixel size
freq_bu	Frequency of occurences (%) of builtup area from RF based land cover map derived on Sentinel-2 imagery
freq_bl	Frequency of occurences (%) of bare land from RF based land cover map derived on Sentinel-2 imagery
freq-wb	Frequency of occurences (%) of water body from RF based land cover map derived on Sentinel-2 imagery

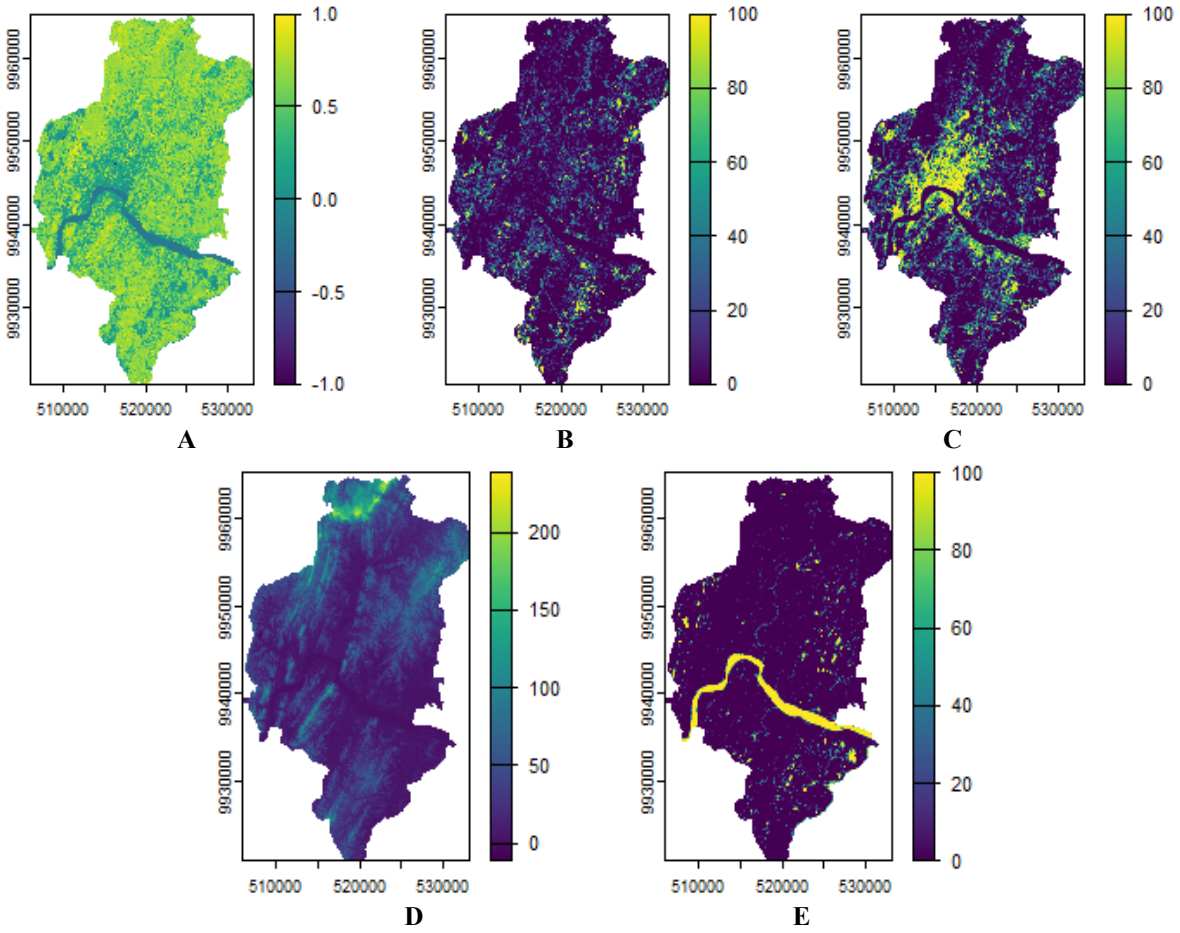

Figure 3. Variables selected from the multicollinearity test prior to GLM-based flood susceptibility model building were: A. EVI, B. bare land, C. Built-up, D. Elevation, and E. Water body

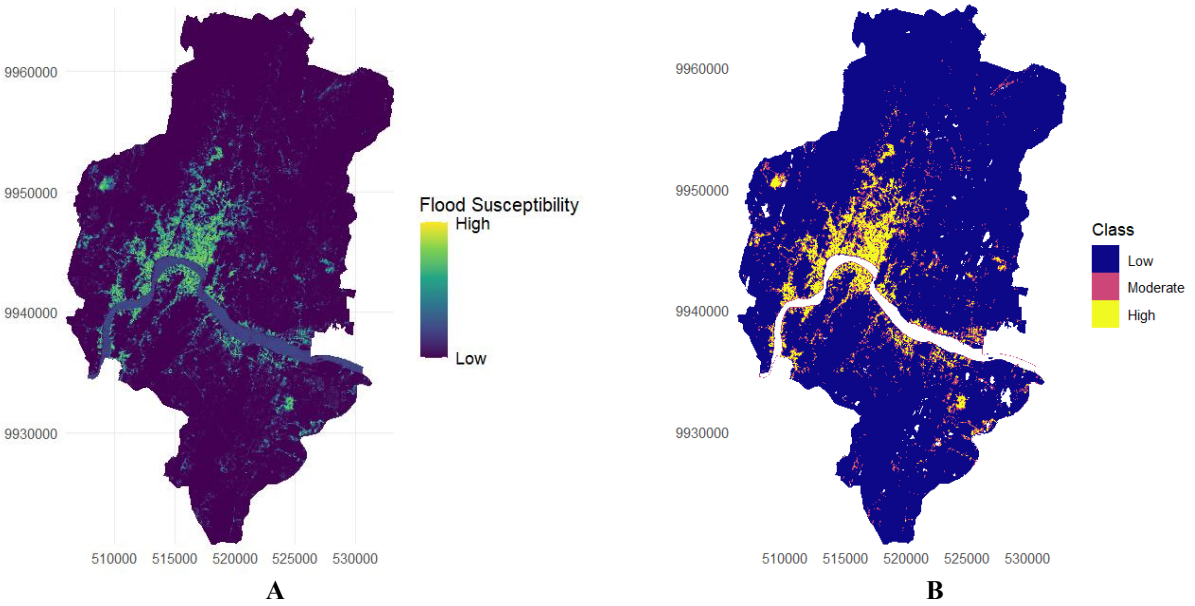

Figure 4. Flood susceptibility maps for Samarinda, Indonesia, generated from the best minimal GLM. A. spatial distribution of continuous predicted flood susceptibility, where higher values occur along the Mahakam River corridor and central-western zones and lower values occur in the southern and peripheral parts of the city; B. The same prediction surface was reclassified into three classes (low, moderate, high) using Jenks natural breaks for descriptive area-based summarization

Model performance was evaluated using a ROC curve (Figure 5), yielding an AUC of 0.959 on the test dataset. Sensitivity and specificity were calculated at the optimal threshold: the optimal threshold was 0.047, with sensitivity = 1.00 and specificity = 0.844. Model performance was further evaluated using spatial block cross-validation, yielding a mean AUC of 0.961 (SD=0.025) across five folds, with mean sensitivity = 0.977 and mean specificity = 0.902. The VIF values in the final model are EVI =1.103, elevation = 1.006, and built-up area = 1.106.

Discussion

The flood susceptibility model in this study was constructed using environmental variables obtained from open-source data (results in Table 2 and spatial predictions in Figure 4). The model highlights the relationship between environmental and geographical variables and flooding events in Samarinda, where the variables used include vegetation cover, elevation, and built-up area. The negative association between vegetation cover and flood events indicates that floods tend to occur in areas with minimal vegetation cover. Similar patterns have been documented across tropical cities, particularly in Southeast Asia, where vegetation cover constitutes a critical element of blue-green infrastructure that helps mitigate urban flood risk in rapidly urbanizing landscapes (Hamel and Tan 2022; Garshasbi et al. 2025; Yuanita and Sagala 2025). Vegetation plays a fundamental role in mitigating hydrological disasters, as its presence in a location can reduce the spread of flooding by increasing flow resistance and prolonging the time it takes for flood waves to reach certain areas (Ali et al. 2019; Giovannini et al. 2025). In addition to vegetation, this condition can be exacerbated by topographical factors, as the model confirms that elevation is negatively associated with flooding events, meaning that areas with lower elevations are more susceptible to flooding (Zhang et al. 2023). Effect-size estimates further support this pattern, showing reduced flood odds with higher vegetation cover and elevation, and increased flood odds with greater built-up frequency.

The positive relationship between built-up areas and flooding events is a consequence of urbanization, as the dominance of impervious surfaces hinders water infiltration into the soil. Furthermore, the dominance of impervious surfaces can increase surface runoff accumulation in certain locations. Built-up expansion along riverbanks often fragments and narrows riparian corridors, which reduces corridor continuity and buffering capacity, increases direct runoff connectivity to channels, and can amplify flood susceptibility in adjacent low-lying urban areas (Feng et al. 2021; Castillo-Acosta et al. 2025). Wang et al. (2020) simulated urban expansion and flood risk over the period 1980-2015 and showed that an increase in impervious surfaces increases flood risk by increasing surface runoff, even in moderate rainfall scenarios. Several studies in Southeast Asian cities have reported similar findings, where an increased risk of flooding is often associated with an increase in impervious surfaces (Sugianto et al. 2022; Huang et al. 2024; Garshasbi et al. 2025).

This study does not explicitly discuss civil infrastructure aspects but focuses on land cover and topography variables in predicting flood vulnerability. However, the expansion of impervious surfaces as part of urbanization should ideally be accompanied by improvements in civil infrastructure, such as drainage systems, to prevent excessive surface runoff (Zhou et al. 2019; Zhang et al. 2024). Simulations conducted by Bibi et al. (2023) show that poor drainage systems are not effective enough in reducing flood risk. On the other hand, drainage alone is also insufficient to mitigate the risk of flooding in an area. A number of previous studies have revealed that vegetation cover plays an important role in reducing flood risk, in addition to the existence of a drainage system (Fletcher et al. 2015; Mell 2017; Machado et al. 2019; Sugianto et al. 2022). In this context, urban vegetation, buffer forests along riverbanks, or riparian green belts within cities can be viewed as part of green infrastructure within a broader landscape management framework (Carter et al. 2018; Liu and Zhang 2025; Xiao et al. 2025). In practical terms, the resulting flood susceptibility map can serve as spatial input for prioritizing segments of riparian corridors that require vegetation reinforcement and land use control.

The spatial prediction visualization of the model shows that flood-susceptible areas are concentrated along the Mahakam River and in the northern part of the city, namely the center of Samarinda City. This pattern is in line with the character of Samarinda's urban landscape, which is dominated by flat topography and extensive built-up areas compared to vegetation cover in the city center, reflecting the general character of urban environments (Nowak and Greenfield 2020; Anwar et al. 2021; Bapperida Kota Samarinda 2024; Malkoç 2024).

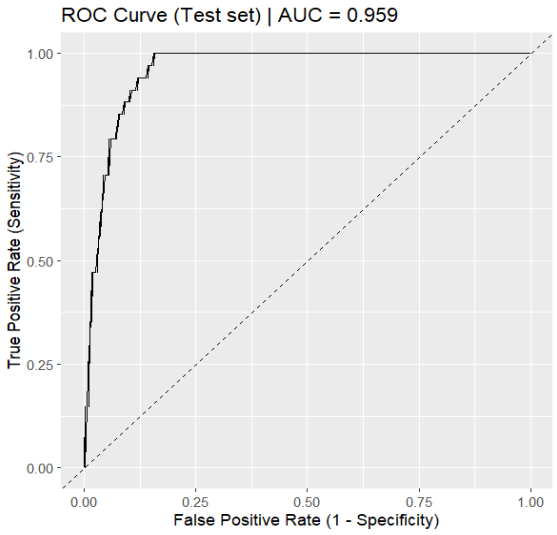

Figure 5. ROC curve of the flood susceptibility model showing an AUC value of 0.959, indicating good model performance

In addition to the city center, the limited vegetation cover around the riverbanks also contributes to high flood susceptibility. The Jenks reclassification provides a descriptive summary of areal extent, indicating that high susceptibility occupies 32.78 km² (4.74%) of the study area, while moderate susceptibility covers 40.92 km² (5.92%) and low susceptibility dominates 617.28 km² (89.33%). Despite its smaller areal proportion, the high-susceptibility class is spatially concentrated along river corridors and low-lying urban zones, making it relevant for prioritizing riparian green-belt reinforcement and land-use control.

Forestry management implications follow directly from this prioritization. High-susceptibility corridor segments can be treated as priority restoration zones where urban riparian forest continuity and buffering functions need to be strengthened through targeted revegetation and protection. Restoration strategies can focus on improving riparian belt continuity, increasing canopy closure, and promoting multi-strata vegetation structure to enhance surface roughness and infiltration capacity during high-flow events (Kiss and Fehérváry 2023; Rahman et al. 2023). Flooding in Samarinda is not only triggered by rainfall but also by fluctuations in the tides of the Mahakam River (Setiawan et al. 2020). Urban riparian forests and vegetated river corridors are important areas for flood mitigation because they can slow surface runoff and increase water infiltration into the soil (Croke et al. 2017; Olokeogun et al. 2020; Viezzer et al. 2022; Kiss and Fehérváry 2023; Vilca-Campana et al. 2025).

Riparian mitigation capacity depends not only on the presence of vegetation but also on structural characteristics such as belt width, canopy closure (canopy density), vertical stratification, and understory density, which jointly control rainfall interception, infiltration opportunity, and hydraulic roughness during high flows (Rahman et al. 2023). Wider and more continuous riparian belts generally provide greater buffering and storage functions, while dense woody and understory structure can increase flow resistance and reduce flow velocities across floodplains and along channel margins (Kiss and Fehérváry 2023). Given that the vegetation predictors in this study (EVI) represent landscape-scale greenness rather than riparian width or canopy density explicitly, the high-susceptibility river-corridor segments are interpreted as priority areas where riparian structure and continuity may be degraded and thus warrant targeted strengthening (Valera et al. 2019). This study primarily captures macro-scale vegetation structure (landscape greenness and cover patterns) rather than micro-scale riparian stand structure measured in the field. Further work is needed to quantify riparian width, canopy density or closure, understory and stem density, and vertical stratification through on-site surveys to better explain mechanisms and strengthen management recommendations. In addition, the loss of ecological corridors due to urbanization pressures can reduce the capacity of rivers to regulate runoff and retain flow during intense rainfall (Eckermann et al. 2022; Vilca-Campana et al. 2025). Beyond flood mitigation, vegetation-based green infrastructure, particularly in riparian corridors, also maintains habitat quality and green space connectivity that are important for biodiversity and ecosystem resilience for sustainable landscape management (De La Fuente et al. 2018; Boncourt et al. 2024). Thus, integrating environmental considerations into regional planning and development is fundamental to ensuring the sustainability of cities in the future (Gustafsson et al. 2019; Adams et al. 2023).

Indonesia, through Law No. 41 of 1999 concerning Forestry, stipulates that logging is not permitted within 100 meters of riverbanks and 50 meters of tributaries in forest areas. More specifically, Regulation of the Minister of Public Works and Public Housing (PUPR) No. 28 of 2015 concerning the Determination of River Boundaries and Lake Boundaries regulates the boundary distance for embanked and unembanked rivers, both in urban and non-urban areas. The main objective of this regulation is to preserve the ecological function of riverbanks, especially as retention and flood buffer zones. In Samarinda City, the findings of Kedhaton and Krismondo (2024), which show that settlements have developed within 100 m of river channels, indicate increasing pressure on land use in riparian corridors. This situation suggests persistent enforcement challenges, particularly where river boundaries are not clearly managed on the ground and urban development pressures are high. These challenges matter for forestry governance because effective riparian buffer protection depends on consistent land-use control and monitoring, especially in already-occupied segments. The susceptibility map (Figure 4) can be used to delineate corridor segments that should be prioritized for strengthening the riparian green belt and regulating land use, and to inform refinement of boundary zoning in the regional spatial plan. This study does not examine spatial-planning compliance or setback enforcement in depth, but it provides spatial evidence to support more targeted implementation.

To contextualize these results, it is important to acknowledge several limitations of the data and modeling approach, even though the model performs well in identifying areas that are physically susceptible to flooding. The use of open-source environmental covariates and flood reports derived from georeferenced online sources and social media means that the analysis reflects documented flood events rather than comprehensively observed events. Moreover, the covariates are relatively static, so land cover changes over time may not be fully captured. A temporal mismatch may also exist because the flood-event reports represent specific dates, whereas the land-cover and vegetation predictors were derived from a composite period, meaning that local land-cover conditions at the time of a reported flood may differ from the mapped covariates. This mismatch can introduce uncertainty in estimated relationships, particularly in rapidly changing urban areas. From a modeling perspective, the correlational framework using a presence-pseudo-absence design in urban landscapes does not explicitly incorporate dynamic hydrological drivers such as rainfall intensity, backwater effects due to tides, or drainage capacity. Consequently, the resulting map is best interpreted as relative vulnerability

based on environmental indicators rather than as deterministic predictions for individual rainfall events. Model discrimination was evaluated using both a random split and spatially separated cross-validation to reduce optimistic bias from spatial autocorrelation. Future research should integrate crowd-sourced flood reports with inundation traces derived from Unmanned Aerial Vehicle (UAV) imagery and higher-resolution hydrometeorological data. This would enable more accurate mapping of actual inundation extents and riparian forest conditions, while supporting stronger model evaluation and improved generalization for sustainable urban landscape management and planning.

In conclusion, this study quantifies how vegetation cover and topography shape urban flood susceptibility in Samarinda, Indonesia, using 123 spatially thinned flood occurrences and 1,000 pseudo-absence points within a GLM framework. Flood occurrence decreases with higher vegetation greenness (EVI) and higher elevation, while greater built-up frequency increases flood susceptibility. Model discrimination is strong, with AUC=0.959 under a 70/30 split and mean AUC=0.961±0.025 under spatial block cross-validation, supporting robust separation between flood-susceptible and non-susceptible locations. Spatial predictions indicate that high susceptibility is concentrated along river corridors and low-lying urban zones, highlighting priority areas for urban riparian green-belt reinforcement and land-use control. These outputs can be used as considerations for urban forestry planning, including prioritizing riparian forest conservation and restoration within urban river corridors as part of flood-risk mitigation and landscape governance. Future work should incorporate rainfall intensity, drainage capacity, and time-series land-cover dynamics to strengthen event-based inference and support operational flood-risk planning.

ACKNOWLEDGEMENTS

We would like to thank Muhammad Rosyid Ridho for his editorial input towards the refinement of this article. We also wish to express our gratitude for the availability of open-source environmental data and online platforms that facilitated the spatial analysis in this study. Our appreciation further extends to colleagues and collaborators who provided constructive feedback during manuscript preparation.

REFERENCES

Adams C, Frantzeskaki N, Moglia M. 2023. Mainstreaming nature-based solutions in cities: A systematic literature review and a proposal for facilitating urban transitions. Land Use Policy 130: 106661. https://doi.org/10.1016/j.landusepol.2023.106661.

Agus F, Prafanto A, Kamil ZA. 2023. Detecting land use land cover using supervised maximum likelihood algorithm on spatiotemporal imagery in Samarinda, Indonesia. IOP Conf Ser Earth Environ Sci 1266 (1): 012085. https://doi.org/10.1088/1755-1315/1266/1/012085.

Agus F, Rahman MMN, Kamil ZA, Gifari OI. 2025. Urban flood modeling using remote sensing technology and 3D simulation: An innovative approach to risk management. Proc Intl Conf Trop Stud Appl 263: 48-60. https://doi.org/10.2991/978-94-6463-732-86.

Aiello-Lammens ME, Boria RA, Radosavljevic A, Vilela B, Anderson, RP. 2015. spThin: An R package for spatial thinning of species occurrence records for use in ecological niche models. Ecography 38 (5): 541-545. https://doi.org/10.1111/ecog.01132.

Ali A, Pasha GA, Ghani U, Ahmed A, Abbas FM. 2019. Investigating role of vegetation in protection of houses during floods. Civ Eng J 5 (12): 2598-2613. https://doi.org/10.28991/cej-2019-03091436.

Amri M, Jamalianuri, Delphia R. 2020. Urban Analysis Report. Climate Resilient and Inclusive Cities (CRIC) Project, Jakarta. [Indonesian]

Anwar Y, Setyasih I, Ningrum MVR. 2021. Multi-ethnic communities adaptation to flooding in the North Samarinda Sub-district, Samarinda City, East Kalimantan Province, Indonesia. IOP Conf Ser Earth Environ Sci 683 (1): 012079. https://doi.org/10.1088/1755-1315/683/1/012079.

Anys M, Weiler M. 2024. Rainfall interception by urban trees: Event characteristics and tree morphological traits. Hydrol Proces 38 (4): e15146. https://doi.org/10.1002/hyp.15146.

Austin M. 2007. Species distribution models and ecological theory: A critical assessment and some possible new approaches. Ecol Model 200 (1-2) : 1-19. https://doi.org/10.1016/j.ecolmodel.2006.07.005.

Bagan H, Yamagata Y. 2015. Analysis of urban growth and estimating population density using satellite images of nighttime lights and land-use and population data. GISci Remote Sens 52 (6): 765-780. https://doi.org/10.1080/15481603.2015.1072400.

Bapperida Kota Samarinda. 2024. Analisis Data dan Informasi untuk Penyusunan Kebijakan Perencanaan Pembangunan Daerah Tahun 2024. Badan Perencanaan Pembangunan, Riset dan Inovasi Daerah Kota Samarinda, Samarinda. [Indonesian]

Barbet-Massin M, Jiguet F, Albert CH, Thuiller W. 2012. Selecting pseudo-absences for species distribution models: How, where and how many? Method Ecol Evol 3 (2): 327-338. https://doi.org/10.1111/j.2041-210x.2011.00172.x.

Berland A, Shiflett SA, Shuster WD, Garmestani AS, Goddard HC, Herrmann DL, Hopton ME. 2017. The role of trees in urban stormwater management. Landsc Urban Plan 162: 167-177. https://doi.org/10.1016/j.landurbplan.2017.02.017.

Bhaskara BE, Pratomo RA. 2023. Perkembangan fenomena urban *heat island* di Kota Samarinda. Jurnal Wilayah dan Lingkungan 11 (1): 22-35. https://doi.org/10.14710/jwl.11.1.22-35. [Indonesian]

Bibi TS, Reddythta D, Kebebew AS. 2023. Assessment of the drainage systems performance in response to future scenarios and flood mitigation measures using stormwater management model. City Environ Interac 19: 100111. https://doi.org/10.1016/j.cacint.2023.100111.

Blum AG, Ferraro PJ, Archfield SA, Ryberg KR. 2020. Causal effect of impervious cover on annual flood magnitude for the United States. Geophys Res Lett 47 (5): e2019GL086480. https://doi.org/10.1029/2019gl086480.

BMKG. 2021. Peta Rata-Rata Curah Hujan dan Hari Hujan Periode 1991-2020 Indonesia. Pusat Informasi Perubahan Iklim BMKG, Jakarta. [Indonesian]

Boncourt E, Bergès L, Alp M, Dupont B, Herviault T, Evette A. 2024. Riparian habitat connectivity restoration in an anthropized landscape: A multi-species approach based on landscape graph and soil bioengineering structures. Environ Manag 73 (6): 1247-1264. https://doi.org/10.1007/s00267-024-01959-5.

Boria RA, Olson LE, Goodman SM, Anderson RP. 2014. Spatial filtering to reduce sampling bias can improve the performance of ecological niche models. Ecol Model 275: 73-77. https://doi.org/10.1016/j.ecolmodel.2013.12.012.

Brown JM, Yelland MJ, Pullen T, Silva E, Martin A, Gold I, Whittle L, Wisse P. 2021. Novel use of social media to assess and improve coastal flood forecasts and hazard alerts. Sci Rep 11 (1): 13727. https://doi.org/10.1038/s41598-021-93077-z.

Brun P, Thuiller W, Chauvier Y, Pellissier L, Wüest RO, Wang Z, Zimmermann NE. 2020. Model complexity affects species distribution projections under climate change. J Biogeogr 47 (1): 130-142. https://doi.org/10.1111/jbi.13734.

Cao Y, Natuhara Y. 2019. Effect of urbanization on vegetation in riparian area: Plant communities in artificial and semi-natural habitats. Sustainability 12 (1): 204. https://doi.org/10.3390/su12010204.

Carter JG, Handley J, Butlin T, Gill S. 2018. Adapting cities to climate change - Exploring the flood risk management role of green infrastructure landscapes. J Environ Plan Manag 61 (9): 1535-1552. https://doi.org/10.1080/09640568.2017.1355777.

Castillo-Acosta Y, Cárdenas-Pillco B, Chanove-Manrique A. 2025. Assessment of pluvial flood mitigation ecosystem service in a riverside city using the integrated valuation of ecosystem services and tradeoffs model for ecological corridor mapping. Water 17 (2): 143. https://doi.org/10.3390/w17020143.

Crawley MJ. 2013. The R book (Second edition). Wiley, Hoboken.

Croke J, Thompson C, Fryirs K. 2017. Prioritising the placement of riparian vegetation to reduce flood risk and end-of-catchment sediment yields: Important considerations in hydrologically-variable regions. J Environ Manag 190: 9-19. https://doi.org/10.1016/j.jenvman.2016.12.046.

Dasallas L, An H, Lee S. 2024. Providing solutions for data scarcity in urban flood modeling through sensitivity analysis and DEM modifications. J Hydroinf 26 (2): 459-479. https://doi.org/10.2166/hydro.2024.173.

De La Fuente B, Mateo-Sánchez MC, Rodríguez G, Gastón A, Pérez De Ayala R, Colomina-Pérez D, Melero M, Saura S. 2018. Natura 2000 sites, public forests and riparian corridors: The connectivity backbone of forest green infrastructure. Land Use Policy 75: 429-441. https://doi.org/10.1016/j.landusepol.2018.04.002.

Dharmarathne G, Waduge AO, Bogahawaththa M, Rathnayake U, Meddage DPP. 2024. Adapting cities to the surge: A comprehensive review of climate-induced urban flooding. Res Eng 22: 102123. https://doi.org/10.1016/j.rineng.2024.102123.

Dimaputri AM, Risyadi F, Pratama GNP. 2022. Flood management strategy in Samarinda City, East Kalimantan Province. Jurnal Mantik 6 (2): 1365-1370.

Dowtin AL, Cregg BC, Nowak DJ, Levia DF. 2023. Towards optimized runoff reduction by urban tree cover: A review of key physical tree traits, site conditions, and management strategies. Landsc Urban Plan 239: 104849. https://doi.org/10.1016/j.landurbplan.2023.104849.

Du S, Shi P, Van Rompaey A, Wen J. 2015. Quantifying the impact of impervious surface location on flood peak discharge in urban areas. Nat Hazard 76 (3): 1457-1471. https://doi.org/10.1007/s11069-014-1463-2.

Eckermann TK, Hunt DS, Kinoshita AM. 2022. Impacts of vegetation removal on urban Mediterranean stream hydrology and hydraulics. Hydrology 9 (10): 170. https://doi.org/10.3390/hydrology9100170.

Ehrenfeld JG, Stander EK. 2010. Habitat function in urban riparian zones. In: Aitkenhead-Peterson J, Volder A (eds.). Urban Ecosystem Ecology. Wiley, Hoboken, New Jersey. https://doi.org/10.2134/agronmonogr55.c6.

Ekeanyanwu CV, Bose P, Beavers M, Yuan Y, Obisakin I. 2022. Modeling and mapping flood hazard with a flood risk assessment tool: A case study of Austin, Texas. J Geogr Inf Syst 14 (04): 332-346. https://doi.org/10.4236/jgis.2022.144018.

El-Haddad BA, Youssef AM, Pourghasemi HR, Pradhan B, El-Shater AH, El-Khashab MH. 2021. Flood susceptibility prediction using four machine learning techniques and comparison of their performance at Wadi Qena Basin, Egypt. Nat Hazard 105 (1): 83-114. https://doi.org/10.1007/s11069-020-04296-y.

Etter A, McAlpine CA, Seabrook L, Wilson KA. 2011. Incorporating temporality and biophysical vulnerability to quantify the human spatial footprint on ecosystems. Biol Conserv 144 (5): 1585-1594. https://doi.org/10.1016/j.biocon.2011.02.004.

Farr TG, Rosen PA, Caro E, Crippen R, Duren R, Hensley S, Kobrick M, Paller M, Rodriguez E, Roth L, Seal D, Shaffer S, Shimada J, Umland J, Werner M, Oskin M, Burbank D, Alsdorf D. 2007. The Shuttle Radar Topography Mission. Rev Geophys 45 (2). https://doi.org/10.1029/2005rg000183.

Feng B, Zhang Y, Bourke R. 2021. Urbanization impacts on flood risks based on urban growth data and coupled flood models. Nat Hazards 106 (1): 613-627. https://doi.org/10.1007/s11069-020-04480-0.

Fletcher TD, Shuster W, Hunt WF, Ashley R, Butler D, Arthur S, Trowsdale S, Barraud S, Semadeni-Davies A, Bertrand-Krajewski JL, Mikkelsen PS, Rivard G, Uhl M, Dagenais D, Viklander M. 2015. SUDS, LID, BMPs, WSUD and more - The evolution and application of terminology surrounding urban drainage. Urban Water J 12 (7): 525-542. https://doi.org/10.1080/1573062x.2014.916314.

Fowler HJ, Lenderink G, Prein AF, Westra S, Allan RP, Ban N, Barbero R, Berg P, Blenkinsop S, Do HX, Guerreiro S, Haerter JO, Kendon EJ, Lewis E, Schaer C, Sharma A, Villarini G, Wasko C, Zhang X. 2021. Anthropogenic intensification of short-duration rainfall extremes. Nat Rev Earth Environ 2 (2): 107-122. https://doi.org/10.1038/s43017-020-00128-6.

Fox J, Weisberg S. 2018. An R Companion to Applied Regression (3rd edition). Sage. https://www.john-fox.ca/Companion. https://doi.org/10.32614/CRAN.package.carData.

Garshasbi D, Kitiphaisannon J, Wongbumru T, Thanvisitthpon NT. 2025. Assessment of future urban flood risk of Thailand's bangkok metropolis using geoprocessing and machine learning algorithm. Environ Sustain Indic 25: 100559. https://doi.org/10.1016/j.indic.2024.100559.

Ghosh P, Dewanji A. 2016. Regression analysis of biased case-control data. Ann Inst Stat Math 68 (4): 805-825. https://doi.org/10.1007/s10463-015-0511-3.

Ghozali A, Rizki AFF, Mustofa U. 2024. Spatial characterization of flood intensity over the drainage condition of East Sempaja Village, Samarinda. Jurnal Presipitasi Media Komunikasi dan Pengembangan Teknik Lingkungan 21 (3): 917-935. https://doi.org/10.14710/presipitasi.v21i3.917-935.

Giovannini MRM, Lama GFC, Scopetani L, Francalanci S, Signorile A, Saracino R, Preti F. 2025. Evaluating the impacts of riparian plants on flood hazard within vegetated rivers. J Flood Risk Manag 18 (2): e70063. https://doi.org/10.1111/jfr3.70063.

Gomez C, Williams AJ, Nicol SJ, Mellin C, Loeun KL, Bradshaw CJA. 2015. Species distribution models of tropical deep-sea snappers. Plos One 10 (6): e0127395. https://doi.org/10.1371/journal.pone.0127395.

Gunawan A, Ariwibowo D, Permana AU, Romadhon WC, Pratama IP. 2013. Geological Investigation about Flood in Samarinda and Preventation. The 42th IAGI Ann Convent Exhibit Proc. PIT IAGI. Medan 2013.

Günlü A, Başkent EZ, Kadıoğulları Aİ, Altun L. 2009. Forest site classification using Landsat 7 ETM data: A case study of Maçka-Ormanüstü forest, Turkey. Environ Monit Assess 151 (1): 93-104. https://doi.org/10.1007/s10661-008-0252-3.

Guo S, Su C, Saito K, Cheng J, Terada T. 2019. Bird communities in urban riparian areas: Response to the local- and landscape-scale environmental variables. Forests 10 (8): 683. https://doi.org/10.3390/f10080683.

Gustafsson S, Hermelin B, Smas L. 2019. Integrating environmental sustainability into strategic spatial planning: the importance of management. J Environ Plan Manag 62 (8): 1321-1338. https://doi.org/10.1080/09640568.2018.1495620.

Hamel P, Tan L. 2022. Blue-green infrastructure for flood and water quality management in Southeast Asia: Evidence and knowledge gaps. Environ Manag 69 (4): 699-718. https://doi.org/10.1007/s00267-021-01467-w.

Hasan S, Al-Hameedawi A, Ismael H. 2022. Supervised Classification Model using Google Earth Engine Development Environment for Wasit Governorate. IOP Conf Ser Earth Environ Sci 961 (1): 012051. https://doi.org/10.1088/1755-1315/961/1/012051.

Hijmans RJ. 2025. terra: Spatial Data Analysis. https://doi.org/10.32614/CRAN.package.terra. [Computer software]

Hirzel AH, Hausser J, Perrin N. 2004. Biomapper (Version 3.1) [Computer software]. Lab. of Conservation Biology, Department of Ecology and Evolution, University of Lausanne, Lausanne. https://www.unil.ch/biomapper.

Huang W, Park E, Wang J, Sophal T. 2024. The changing rainfall patterns drive the growing flood occurrence in Phnom Penh, Cambodia. J Hydrol Reg Stud 55: 101945. https://doi.org/10.1016/j.ejrh.2024.101945.

Imam AUK, Indu MS. 2018. Construction in nature versus nature of construction. In: Sarma AK, Singh VP, Bhattacharjya RK, Kartha SA (eds). Urban Ecology, Water Quality and Climate Change. Springer, Cham. https://doi.org/10.1007/978-3-319-74494-02.

Jacobson CR. 2011. Identification and quantification of the hydrological impacts of imperviousness in urban catchments: A review. J Environ Manag 92 (6): 1438-1448. https://doi.org/10.1016/j.jenvman.2011.01.018.

James G, Witten D, Hastie T, Tibshirani R. 2021. An Introduction to Statistical Learning: With Applications in R. Springer New York, New York. https://doi.org/10.1007/978-1-0716-1418-1.

Kedhaton AS, Krismondo A. 2024. Monitoring the arrangement of riverbank settlements in Samarinda: A case study of the river buffer zone in the Sub-districts of Loa Janan Ilir, Palaran, and Samarinda Seberang. Jurnal Riset Inossa Media Hasil Riset Pemerintahan, Ekonomi dan Sumber Daya Alam 5 (02): 39-51. https://doi.org/10.54902/jri.v5i02.141. [Indonesian]

Kingsbury-Smith L, Willis T, Smith M, Boisgontier H, Turner D, Hirst J, Kirkby M, Klaar M. 2023. Evaluating the effectiveness of land use

management as a natural flood management intervention in reducing the impact of flooding for an upland catchment. Hydrol Process 37 (4): e14863. https://doi.org/10.1002/hyp.14863.

Kiss T, Fehérváry I. 2023. Increased riparian vegetation density and its effect on flow conditions. Sustainability 15 (16): 12615. https://doi.org/10.3390/su151612615.

Liu J, Xiong J, Chen Y, Sun H, Zhao X, Tu F, Gu Y. 2023. A new avenue to improve the performance of integrated modeling for flash flood susceptibility assessment: Applying cluster algorithms. Ecol Indic 146: 109785. https://doi.org/10.1016/j.ecolind.2022.109785.

Liu N, Zhang F. 2025. Urban green spaces and flood disaster management: Toward sustainable urban design. Front Public Health 13: 1583978. https://doi.org/10.3389/fpubh.2025.1583978.

Lobo JM, Tognelli MF. 2011. Exploring the effects of quantity and location of pseudo-absences and sampling biases on the performance of distribution models with limited point occurrence data. J Nat Conserv 19 (1): 1-7. https://doi.org/10.1016/j.jnc.2010.03.002.

Lombardo M, Totaro V, Chiaravalloti F, Petrucci O. 2025. Street-scale hydrodynamic estimation from social media videos: A systematic approach to urban floods data collection. Intl J Dis Risk Reduct 122: 105419. https://doi.org/10.1016/j.ijdrr.2025.105419.

Machado RAS, Oliveira AG, Lois-González RC. 2019. Urban ecological infrastructure: The importance of vegetation cover in the control of floods and landslides in Salvador / Bahia, Brazil. Land Use Policy 89: 104180. https://doi.org/10.1016/j.landusepol.2019.104180.

Malkoç E. 2024. City-wide assessment of urban tree cover and land-cover changes in Edirne using web-based tools. Intl J Appl Earth Observ Geoinf 132: 103997. https://doi.org/10.1016/j.jag.2024.103997.

McGrane SJ. 2016. Impacts of urbanisation on hydrological and water quality dynamics, and urban water management: A review. Hydrol Sci J 61 (13): 2295-2311. https://doi.org/10.1080/02626667.2015.1128084.

Meili N, Acero JA, Peleg N, Manoli G, Burlando P, Fatichi S. 2021. Vegetation cover and plant-trait effects on outdoor thermal comfort in a tropical city. Build Environ 195: 107733. https://doi.org/10.1016/j.buildenv.2021.107733.

Mell IC. 2017. Green infrastructure: Reflections on past, present and future praxis. Landsc Res 42 (2): 135-145. https://doi.org/10.1080/01426397.2016.1250875.

Neuhaus J, McCulloch C. 2011. Generalized linear models. WIREs Comput Stat 3 (5): 407-413. https://doi.org/10.1002/wics.175.

Nkwunonwo UC, Whitworth M, Baily B. 2020. A review of the current status of flood modelling for urban flood risk management in the developing countries. Sci Afr 7: e00269. https://doi.org/10.1016/j.sciaf.2020.e00269.

Nowak DJ, Greenfield EJ. 2020. The increase of impervious cover and decrease of tree cover within urban areas globally (2012-2017). Urban For Urban Green 49: 126638. https://doi.org/10.1016/j.ufug.2020.126638.

Nunes CHM, Endreny TA, Carvalho FA. 2025. With great ecosystem services comes great responsibility: Benefits provided by urban vegetation in Brazilian cities. Plants 14 (3): 392. https://doi.org/10.3390/plants14030392.

Olokeogun OS, Ayanlade A, Popoola OO. 2020. Assessment of riparian zone dynamics and its flood-related implications in Eleyele area of Ibadan, Nigeria. Environ Syst Res 9 (1): 6. https://doi.org/10.1186/s40068-020-00167-4.

Pallathadka A, Sauer J, Chang H, Grimm NB. 2022. Urban flood risk and green infrastructure: Who is exposed to risk and who benefits from investment? A case study of three U.S. Cities. Landsc Urban Plan 223: 104417. https://doi.org/10.1016/j.landurbplan.2022.104417.

Phan TN, Kuch V, Lehnert LW. 2020. Land cover classification using Google Earth Engine and Random Forest classifier-The role of image composition. Remote Sens 12 (15): 2411. https://doi.org/10.3390/rs12152411.

Pickett STA, Cadenasso ML, Grove JM, Nilon CH, Pouyat RV, Zipperer WC, Costanza R. 2001. Urban ecological systems: Linking terrestrial ecological, physical, and socioeconomic components of metropolitan areas. Ann Rev Ecol Syst 32 (1): 127-157. https://doi.org/10.1146/annurev.ecolsys.32.081501.114012.

Rahman MA, Pawijit Y, Xu C, Moser-Reischl A, Pretzsch H, Rötzer T, Pauleit S. 2023. A comparative analysis of urban forests for storm-water management. Sci Rep 13 (1): 1451. https://doi.org/10.1038/s41598-023-28629-6.

Robin X, Turck N, Hainard A, Tiberti N, Lisacek F, Sanchez JC, Müller M. 2011. pROC: An open-source package for R and S+ to analyze and compare ROC curves. BMC Bioinfor 12 (1): 77. https://doi.org/10.1186/1471-2105-12-77.

Rudin C. 2019. Stop explaining black box machine learning models for high stakes decisions and use interpretable models instead. Nat Mach Intell 1 (5): 206-215. https://doi.org/10.1038/s42256-019-0048-x.

Setiawan H, Jalil M, Purwadi,F, Adios C, Brata AW, Jufda AS. 2020. Analisis penyebab banjir di Kota Samarinda. Jurnal Geografi Gea 20 (1): 39-43. https://doi.org/10.17509/gea.v20i1.22021. [Indonesian]

Singh VP. 2018. Sustainable urban ecosystems: Problems and perspectives. In: Sarma AK, Singh VP, Bhattacharjya RK, Kartha SA (eds.). Urban Ecology, Water Quality and Climate Change. Springer, Cham. https://doi.org/10.1007/978-3-319-74494-01.

Smith L, Liang Q, James P, Lin W. 2017. Assessing the utility of social media as a data source for flood risk management using a real-time modelling framework. J Flood Risk Manag 10 (3): 370-380. https://doi.org/10.1111/jfr3.12154.

Song P, Guo J, Xu E, Mayer AL, Liu C, Huang J, Tian G, Kim G. 2020. Hydrological effects of urban green space on stormwater runoff reduction in Luohe, China. Sustainability 12 (16): 6599. https://doi.org/10.3390/su12166599.

Stutter M, Baggaley N, Huallacháin DÓ, Wang C. 2021. The utility of spatial data to delineate river riparian functions and management zones: A review. Sci Total Environ 757: 143982. https://doi.org/10.1016/j.scitotenv.2020.143982.

Su M, Zheng Y, Hao Y, Chen Q, Chen S, Chen Z, Xie H. 2018. The influence of landscape pattern on the risk of urban water-logging and flood disaster. Ecol Indic 92: 133-140. https://doi.org/10.1016/j.ecolind.2017.03.008.

Sugianto S, Deli A, Miswar E, Rusdi M, Irham M. 2022. The effect of land use and land cover changes on flood occurrence in Teunom Watershed, Aceh Jaya. Land 11 (8): 1271. https://doi.org/10.3390/land11081271.

Tabari H. 2020. Climate change impact on flood and extreme precipitation increases with water availability. Sci Rep 10 (1): 13768. https://doi.org/10.1038/s41598-020-70816-2.

Tang Z, Wang P, Li Y, Sheng Y, Wang B, Popovych N, Hu T. 2024. Contributions of climate change and urbanization to urban flood hazard changes in China's 293 major cities since 1980. J Environ Manag 353: 120113. https://doi.org/10.1016/j.jenvman.2024.120113.

Tong R, Yesson C, Yu J, Luo Y, Zhang L. 2023. Key factors for species distribution modeling in benthic marine environments. Front Mar Sci 10: 1222382. https://doi.org/10.3389/fmars.2023.1222382.

Tsumita N, Piyapong S, Kaewkluengklom R, Jaensirisak S, Fukuda A. 2025. Flood susceptibility mapping of urban flood risk: Comparing autoencoder multilayer perceptron and logistic regression models in Ubon Ratchathani, Thailand. Nat Hazards 121 (15): 17833-17867. https://doi.org/10.1007/s11069-025-07494-8.

Valera CA, Pissarra TCT, Filho MVM, Valle Júnior RFD, Oliveira CF, Moura JP, Sanches Fernandes LF, Pacheco FAL. 2019. The buffer capacity of riparian vegetation to control water quality in anthropogenic catchments from a legally protected area: A critical view over the Brazilian New Forest Code. Water 11 (3): 549. https://doi.org/10.3390/w11030549.

Varra G, Della Morte R, Tartaglia M, Fiduccia A, Zammuto A, Agostino I, Booth CA, Quinn N, Lamond JE, Cozzolino L. 2024. Flood susceptibility assessment for improving the resilience capacity of railway infrastructure networks. Water 16 (18): 2592. https://doi.org/10.3390/w16182592.

Viezzer J, Schmidt MAR, Dos Reis ARN, Freiman FP, De Moraes EN, Biondi D. 2022. Restoration of urban forests to reduce flood susceptibility: A starting point. Intl J Dis Risk Reduct 74: 102944. https://doi.org/10.1016/j.ijdrr.2022.102944.

Vilca-Campana K, Carrasco-Valencia L, Iruri-Ramos C, Cárdenas-Pillco B, Escudero A, Chanove-Manrique A. 2025. Improving urban flood resilience: Urban flood risk mitigation assessment using a geospatial model in the urban section of a river corridor. Water 17 (7): 1047. https://doi.org/10.3390/w17071047.

Wang Y, Xie X, Liang S, Zhu B, Yao Y, Meng S, Lu C. 2020. Quantifying the response of potential flooding risk to urban growth in Beijing. Sci Total Environ 705: 135868. https://doi.org/10.1016/j.scitotenv.2019.135868.

Wei T, Simko V. 2024. R Package "Corrplot": Visualization of a Correlation Matrix (Version 0.95) [Computer software]. https://github.com/taiyun/corrplot.

Wickham H, François R, Henry L, Müller K, Vaughan D. 2023. dplyr: A Grammar of Data Manipulation. R package version 1.2.0. https://dplyr.tidyverse.org. [Computer software]

Wickham H. 2016. ggplot2: Elegant Graphics for Data Analysis. Springer, Cham. https://doi.org/10.1007/978-3-319-24277-4.

Widayati R. 2018. Rencana lansekap tepian Sungai Mahakam Samarinda Sebrang. Jurnal Teknologi Sipil 2 (1): 8-17. https://dx.doi.org/10.30872/ts.v2i1.2146. [Indonesian]

Wu J, Sha W, Zhang P, Wang Z. 2020. The spatial non-stationary effect of urban landscape pattern on urban waterlogging: A case study of Shenzhen City. Sci Rep 10 (1): 7369. https://doi.org/10.1038/s41598-020-64113-1.

Xiao L, Mokhtar NA, Sulaiman MKAM, Khalit NA. 2025. Enhancing urban sustainability through green infrastructure: Spatiotemporal analysis of green space and forest coverage in Sichuan (2002-2022). Sustainability 17 (11): 5135. https://doi.org/10.3390/su17115135.

Yuanita CN, Sagala S. 2025. Blue-green infrastructure in Jakarta's fringe: An analysis of accessibility to blue-green spaces as a flood solution in Bekasi City. Intl J Dis Risk Reduct 121: 105425. https://doi.org/10.1016/j.ijdrr.2025.105425.

Zhang X, Kang A, Ye M, Song Q, Lei X, Wang H. 2023. Influence of terrain factors on urban pluvial flooding characteristics: A case study of a small watershed in Guangzhou, China. Water 15 (12): 2261. https://doi.org/10.3390/w15122261.

Zhang X, Zhang L, Wang Y, Shao Y, Daniels B, Roß-Nickoll M, Chen Z. 2022. Pollinators and urban riparian vegetation: Important contributors to urban diversity conservation. Environ Sci Eur 34 (1): 78. https://doi.org/10.1186/s12302-022-00661-9.

Zhang Y, Wang E, Gong Y. 2024. A structural optimization of urban drainage systems: An optimization approach for mitigating urban floods. Water 16 (12): 1696. https://doi.org/10.3390/w16121696.

Zhou Q, Leng G, Su J, Ren Y. 2019. Comparison of urbanization and climate change impacts on urban flood volumes: Importance of urban planning and drainage adaptation. Sci Total Environ 658: 24-33. https://doi.org/10.1016/j.scitotenv.2018.12.184.

Zhou W, Cadenasso M, Schwarz K, Pickett S. 2014. Quantifying spatial heterogeneity in urban landscapes: Integrating visual interpretation and object-based classification. Remote Sens 6 (4): 3369-3386. https://doi.org/10.3390/rs6043369.

Zhou Z, Smith JA, Yang L, Baeck ML, Chaney M, Veldhuis MT, Deng H, Liu S. 2017. The complexities of urban flood response: Flood frequency analyses for the Charlotte metropolitan region. Water Resour Res 53 (8): 7401-7425. https://doi.org/10.1002/2016wr019997.